Templates of expected measurement uncertainties for average prompt and total fission neutron multiplicities

Neudecker, Denise
Carlson, A.
Croft, S.
Devlin, Matthew James
Kelly, Keegan John
Lovell, Amy Elizabeth
Marini, Paola
Taieb, J.

To be published in: EPJ Nuclear Sciences & Technologies

DOI to publisher's version: 10.1051/epjn/2023016

EPJ Nuclear Sci. Technol. **9**, 30 (2023)

https://doi.org/10.1051/epjn/2023016

EPJ Nuclear Sciences & Technologies

Available online at:
https://www.epj-n.org

Templates of Expected Measurement Uncertainties: a CSEWG Effort, Cyrille De Saint Jean and Denise Neudecker (Guest editors)

REGULAR ARTICLE

OPEN ACCESS

Templates of expected measurement uncertainties for average prompt and total fission neutron multiplicities

Denise Neudecker[1,*], Allan D. Carlson[2], Stephen Croft[3], Matthew Devlin[1], Keegan J. Kelly[1], Amy E. Lovell[1], Paola Marini[4,5], and Julien Taieb[4,6]

[1] Los Alamos National Laboratory, Los Alamos, New Mexico 87545, USA
[2] National Institute of Standards and Technology, Gaithersburg, MD 20899-8463, USA
[3] Lancaster University, Lancaster LA1 4YW, UK
[4] CEA, DAM, DIF, F-91297 Arpajon, France
[5] Univ. Bordeaux, LP2I, UMR5797, CNRS, F-33170 Gradignan, France
[6] Université Paris-Saclay, CEA, LMCE, 91680 Bruyères-le-Châtel, France

Received: 23 March 2023 / Received in final form: 18 July 2023 / Accepted: 30 August 2023

Abstract. In this paper, we provide templates of measurement uncertainty sources expected to appear for average prompt- and total-fission neutron multiplicities, $\overline{\nu}_p$ and $\overline{\nu}_t$, for the following measurement types: absolute manganese-bath experiments for $\overline{\nu}_t$, absolute and ratio liquid-scintillator measurements for $\overline{\nu}_p$. These templates also suggest a typical range of these uncertainties and their correlations based on a survey of available experimental data, associated literature, and feedback from experimentalists. In addition, the information needed to faithfully include the associated experimental data into the nuclear-data evaluation process is provided.

1 Introduction

The average prompt-fission neutron multiplicity, $\overline{\nu}_p$, of an actinide is the average number of neutrons emitted promptly following fission of that nucleus and before the onset of β-decay. The average total-fission neutron multiplicity, $\overline{\nu}_t$, differs from $\overline{\nu}_p$ in that it also includes delayed neutrons. These observables can be measured for both spontaneous, e.g., the Neutron Data Standard (NDS) ^{252}Cf(sf) $\overline{\nu}_t$, or neutron-induced fission, e.g., the ^{235}U(n,f) $\overline{\nu}_p$ as a function of incident-neutron energy. Neutron multiplicities can also be measured as a function of other quantities, for instance, fission-fragment mass, charge, or total kinetic energy. Here, we focus on $\overline{\nu}_p$ and $\overline{\nu}_t$. The variable $\overline{\nu}$ is also used as a short version encompassing both $\overline{\nu}_p$ and $\overline{\nu}_t$.

Observations of $\overline{\nu}$ are among those that can be measured to the highest precision, i.e., lowest uncertainty, compared to other nuclear-reaction data, with uncertainties reported as low as 0.3–0.5% [1–8]. Given that many $\overline{\nu}$ measurements are of high precision, these experiments must be carefully documented with regard to data analysis, corrections, and all pertinent uncertainties. Many high-precision measurements are given for ^{252}Cf(sf) $\overline{\nu}_t$ [1–9], thermal constants (^{233,235}U(n,f) $\overline{\nu}_t$ and ^{239,241}Pu(n,f) $\overline{\nu}_t$ as described in [10–18]) and also for incident-neutron energy dependent $\overline{\nu}_p$ and $\overline{\nu}_t$ [14–16,19–26].

In Section 4, templates are provided for $\overline{\nu}$ measurements using the absolute manganese-bath technique for $\overline{\nu}_t$, and absolute and ratio liquid-scintillator technique for $\overline{\nu}_p$; these techniques are described in Section 2 along with information needed to be provided on a particular experiment for nuclear data evaluations in Section 3. The templates on absolute $\overline{\nu}$ measurements were established by analyzing ^{252}Cf(sf) $\overline{\nu}_t$ data sets using information from their literature [2–9,15,27–30] and respective entries in the EXFOR (Experimental Nuclear Reaction Data) database [31–33]. The templates for ratio liquid-scintillator measurements were obtained using information from several ^{239}Pu(n,f) $\overline{\nu}_t$ and $\overline{\nu}_p$ data sets from thermal to 20 MeV incident-neutron energy using their literature and EXFOR entries [12–26,34–42]. Most of these data sets were either measured at thermal energies or above 100 keV. Only scarce experimental information is available in the resonance range, where variations in $\overline{\nu}_p$ have been investigated for ^{235}U(n,f) (negligible variations) and ^{239}Pu(n,f) (significant variations) [43,44]. The experimental information obtained from these analyses was supplemented by reviews on these experiments and associated measurement techniques [1,45–48], while references [11,43,49,50] provided input on $\overline{\nu}_p$ and $\overline{\nu}_t$ evaluations. Section 5 provides a short summary.

* e-mail: dneudecker@lanl.gov

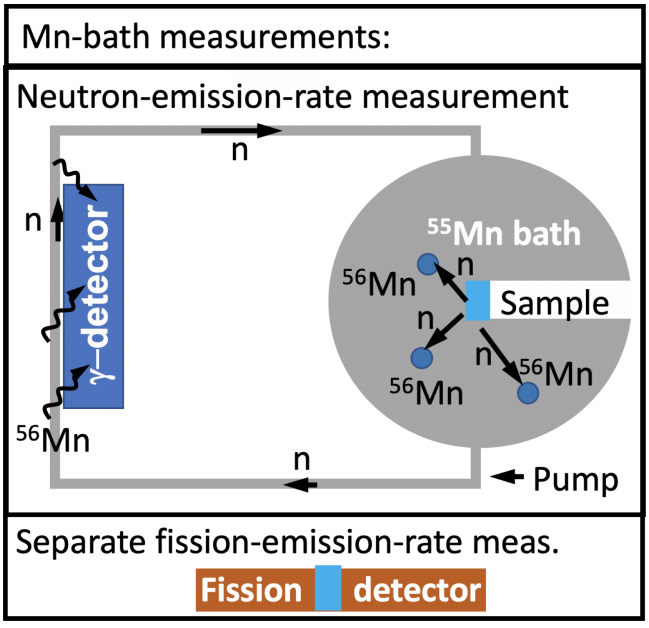

Fig. 1. A schematic drawing of the absolute Mn-bath $\overline{\nu_t}$ measurement type.

2 Measurement types

Three techniques were used for absolute ^{252}Cf(sf) $\overline{\nu}$ measurements: manganese-sulfate baths (Mn baths) [3,5–7,9,11,30], boron piles [4,29] and doped liquid scintillators [1,2,8,15,27]. The differentiation is made according to the neutron-absorbing material, as each of these materials and associated measurement types carry distinct uncertainty sources. Boron-pile measurements will not be discussed here as the template would have been established on only two ^{252}Cf(sf) $\overline{\nu}$ measurements [4,29], too small of a sample size for realistic estimates of typically appearing uncertainty sources. Mainly one ratio-type measurement was encountered in EXFOR entries for ^{239}Pu $\overline{\nu}_p$ and $\overline{\nu}_t$ [12–26,34–42], namely, ratio liquid-scintillator measurements, which will be discussed below. Some $\overline{\nu}_p$ data have also been measured with setups that are traditionally used to determine prompt fission neutron spectra (PFNS), see e.g., [51–54]. To this end, the PFNS is measured via the techniques described in reference [55], extrapolated to span the entire outgoing-neutron energy, E_{out}, range, and then integrated over these energies to yield $\overline{\nu}_p$. Hence, the templates in Tables I and II of [55] apply to this measurement technique along with additional uncertainties for the extrapolation of the PFNS for E_{out} and angular coverage of the neutron detectors. Given that and that only a few data sets use this technique, no separate template is provided.

2.1 Mn-bath measurements

In this type of experiment, $\overline{\nu_t}$ is absolutely determined by measuring the absolute neutron-emission rate, c_n, independently from the fission rate, c_f, (see Fig. 1), and then dividing them

$$\overline{\nu_t} = \frac{c_n}{c_f}. \tag{1}$$

The neutron-emission rate, c_n, is measured by a manganese-sulfate bath. To this end, the sample or detector enclosing it is placed in a re-entrant cavity such that it is located near the center of the bath. The Mn solution is very caustic and is never in contact with the sample or detector. When neutrons are emitted from the sample, some are captured by ^{55}Mn forming radioactive ^{56}Mn. For some measurements, the solution in the bath is continuously stirred and pumped through a tube and back into the bath. Detectors (often NaI scintillators) are located very near (or in a re-entrant well in) that tube, to detect the γ rays from the decay of ^{56}Mn, which yields an estimate of c_n after applying necessary corrections. Non-pumped variants also were undertaken, where detectors were placed on the tank walls. The formal analysis procedure to obtain c_n from this measurement was described in references [30,45] by:

$$c_n = \frac{c_{\text{S}}}{\varepsilon_{\text{Mn}}} \frac{1 + \frac{\sigma_{\text{S}}}{\sigma_{\text{Mn}}(1+G\overline{r}s)} + \frac{N_{\text{H}}\sigma_{\text{H}}}{N_{\text{Mn}}\sigma_{\text{Mn}}(1+G\overline{r}s)}}{(1-L_n)(1-S)(1-O)}, \tag{2}$$

where c_s is the γ-counting rate measured by the Mn bath at saturation (i.e., activity equilibrium) [30,47] with an efficiency ε_{Mn}. Corrections have to be applied for thermalized neutrons captured by sulfur and hydrogen using their respective cross sections, σ_{S} and σ_{H}, in ratio to that of Mn, σ_{Mn}, which can be determined independently. To this end, the ratio of the number of atoms of Mn to H, $\frac{N_{\text{H}}}{N_{\text{Mn}}}$, has to be considered. The ratio of Mn to S is always unity, due to the chemical composition of the bath and, hence, does not appear. No correction has to be applied for thermalized neutrons captured in ^{16}O of the $MnSO_4$ in the bath, as the thermal neutron-capture cross-section of ^{16}O is approximately a factor 10,000 smaller than the Mn cross-section. ^{16}O is also present in the water of the aqueous solution; hence, the O/Mn also depends on the concentration of the solution. Different baths use different concentrations and this should be documented. The term $(1 + G\overline{r}s)$ accounts for the resonance capture of neutrons in Mn, with G the resonance self-shielding factor, $\overline{r}$ the Wescott factor (epithermal flux parameter averaged over the Mn bath) and s being the resonance-activation integral of Mn. The term $(1 - L_n)$ accounts for neutrons leaking from the bath, $(1 - S)$ for neutrons recaptured by the source or material in the cavity, and $(1 - O)$ for those fast neutrons undergoing (n,α) and (n,p) reactions in oxygen in the water or sulfur present in the Mn-bath solution. Mn baths are often calibrated with respect to national standards [48]. The γ detectors measuring decay from ^{56}Mn can be calibrated by adding ^{56}Mn to the solution. The activity can be determined absolutely very accurately making Mn-bath measurements a technique supported by basic radiation metrology. Thermal-neutron absorber impurities need to be known and corrected as described as part of the templates below. The temperature of the bath can also lead to a subtle effect if the pumping heats the water and it is not in thermal equilibrium with environmental temperatures.

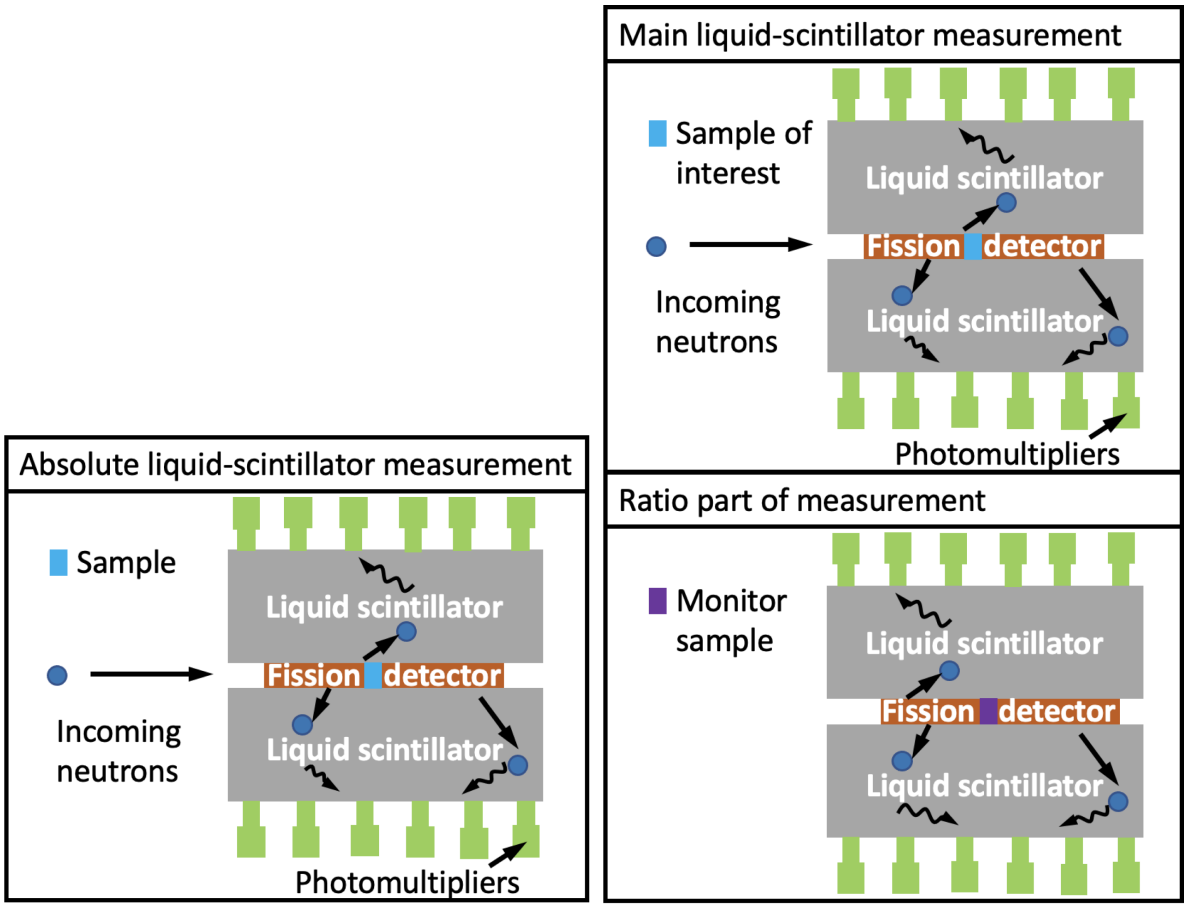

Fig. 2. Schematic drawings of liquid-scintillator $\overline{\nu}$ measurement types. (a) Absolute liquid scintillator, (b) ratio liquid scintillator.

A drawback of the Mn-bath technique is that it requires fairly strong neutron-emission rates. ^{252}Cf naturally lends itself to such a technique, but it is a significant challenge to create deposits of strong enough fission rates that remain amenable to fission counting. However, it is a very important technique as it allows experimentalists to uncover unknown systematic biases in standard techniques, such as the liquid-scintillator technique. The fission rate, c_f, was determined, e.g., by solid-angle counting of fission fragments using Si-surface barrier detectors [9,30], fission-fission coincidence counting [3] or neutron-fission coincidence counting [7]. No explicit equation is given here to derive c_f as it would be different for each of those three measurement techniques.

2.2 Absolute liquid-scintillator measurements

Absolute liquid-scintillator measurements belong to the class of delayed-coincidence measurements [1] and were used to report, e.g., ^{252}Cf(sf) $\overline{\nu}$ measurements [1,2,8,15,27] or also the neutron-multiplicity distribution, $P(\nu)$. In these measurements, a fission detector is placed within a through-tube running through the center of a large liquid scintillator, as shown in Figure 2[1]. When the fission detector is triggered (often by fission fragments), a neutron-counting gate is opened for a defined time (between 30–100 µs across, e.g., the following ratio measurements [12–15,19–23,28,34,35]). During this time, some of the emitted neutrons are captured by the dopant in the scintillator material. The associated capture γ rays cause scintillations that are subsequently detected by photomultipliers. This technique differs from Mn-bath measurements in as far as it is independent of the absolute fission rate as it measures $\overline{\nu}_p$ per detected fission event. The liquid-scintillator material is loaded or doped with gadolinium [1,2,8,19–25] or cadmium [15,26–28]. Both have large neutron-capture cross sections at thermal energies and liberate approximately 6 MeV of γ rays in the capture reaction. These γ rays give an easily detected signal when converted to light in the liquid scintillator. Paraffin scintillators were also used for a few ^{239}Pu $\overline{\nu}$ ratio liquid-scintillator measurements [17,18,39,40]. The analysis of an absolute liquid-scintillator $\overline{\nu}_p$ measurement

[1] To be exact, one does not need to use necessarily a liquid-scintillator neutron detector; one could, for instance, detect neutrons via plastic scintillator bars interlaced with thin Gd sheets, or poly assemblies with large ^{3}He tubes.

can be described by the following equation:

$$\overline{\nu}_p = \frac{c - c_{\mathrm{DG}} - b - c_{ff} - c_{\mathrm{FE}}}{\varepsilon_n \tau}\omega. \quad (3)$$

The photomultipliers convert the scintillator light produced by γ rays from the neutron-capture event in the scintillator into electrons and, hence, in a signal. These counts c are average counts per fission, as these γs are only counted after fission triggered the start of the neutron-counting gate for a limited time. The fission count rate does not appear in this equation, contrary to Mn-bath measurements, because fission is used as a trigger and the desired quantity is the number of neutrons per fission. However, the fission rate must be low enough that neutrons from a not-detected fission event are not measured as part of the next fission-neutron coincidence. The total counts, c, are corrected for (a) γ counts originating from delayed γs due to radioactive decay of the fission fragment, c_{DG}, (b) random background counts in the neutron detector, b, produced by background neutrons not originating from fission, (c) false fission events, c_{ff}, triggered by random coincidences, and (d) counts due to the so-called "French effect", c_{FE} (described in detail as part of Sect. 4). The correction factor, ω, accounts for neutrons resulting from fission of impurity isotopes in the sample, while τ is the dead-time correction. The remaining term is the average scintillator detector efficiency, ε_n, which is obtained by:

$$\varepsilon_n(E_{\mathrm{inc}}) = \epsilon_\gamma \int\int \mathrm{d}E_{\mathrm{out}}\mathrm{d}\theta \epsilon_c(E_{\mathrm{out}},\theta)\chi(E_{\mathrm{inc}},E_{\mathrm{out}}) \times L_n(E_{\mathrm{out}},\theta)a(E_{\mathrm{inc}},E_{\mathrm{out}},\theta)A_t(E_{\mathrm{out}},\theta), \quad (4)$$

where ϵ_γ is the efficiency for detecting γ rays produced in the neutron capture on gadolinium or cadmium. It is assumed to be independent of the neutron energy in reference [1]. The efficiency of the neutron-capture process, $\epsilon_c(E_{\mathrm{out}},\theta)$, is usually calculated via Monte Carlo (MC) codes and depends on nuclear data [1] (cross sections, angular distributions, PFNS), as is the neutron-leakage correction, L_n. Calculations of ϵ_c may also depend on a discrimination threshold to detect the γs. Hence, neutrons that do not produce γs are included in this calculation. The neutron-detector efficiency also requires knowledge of the PFNS, χ, and the angular distribution of fission neutrons, a, which are either simulated or taken from nuclear data. The asymmetry introduced by the through-tube, A_t, also has to be accounted for in the neutron-detector efficiency calculation. The neutron-detector efficiency, ε_n, can also be absolutely measured by means of proton-recoil detectors located in the center of the scintillator, as was done in references [2,15]. These detectors measure the fraction of pulses, C_0, detected by the proton-recoil detector but not by the scintillator as a function of incident-neutron energy. One can then derive ε_n by $(1 - C_0)/(1 - \int\int \mathrm{d}E_{\mathrm{out}}\mathrm{d}\theta L_n(E_{\mathrm{out}},\theta)\chi(E_{\mathrm{inc}},E_{\mathrm{out}})a(E_{\mathrm{inc}},E_{\mathrm{out}},\theta)$, where the denominator is simulated using nuclear data. The derived ε_n can then be compared to equation (4). One can also combine measurements and simulations, by measuring the efficiency for a few energies, while calculations, that were normalized to the measured ε_n, fill in the missing energies [2,4]. This combined approach has the advantage of avoiding the need for absolute simulated values of ε_n. Although equation (4) looks forbidding, in practice, it usually varies only gradually with mean prompt fission neutron energy.

2.3 Ratio liquid-scintillator measurements

These measurements differ from their absolute counterpart in that two measurements are performed. The first measurement determines $\overline{\nu}$ of the desired isotope and is schematically the same as absolute measurements in Figure 2. The second experiment uses the same liquid scintillator and determines its efficiency by measuring a reference (or monitor) sample. This monitor is often ^{252}Cf and thus no incident-neutron beam is shown in Figure 2. The resulting experimental quantity is then a ratio of $\overline{\nu}$ of the desired and monitor isotopes. The measured ratio relative to monitor m is determined by:

$$\overline{\nu}_p/\overline{\nu}_p^m = \frac{c - c_{\mathrm{DG}} - b - c_{ff}}{c^m - c_{\mathrm{DG}}^m - b^m - c_{ff}^m}\frac{\omega\tau^m}{\omega^m\tau\varepsilon_n'}d, \quad (5)$$

with an additional correction for the thickness of the sample, d, leading to differences in the fission-fragment efficiency for specific fission-fragment pairs that may impact $\overline{\nu}$ [21,56]. This factor does not appear for absolute measurements of ^{252}Cf, as the samples are usually sources of small diameter or thickness, or both. The efficiency, ϵ_n'. changes in the ratio measurement to:

$$\varepsilon_n'(E_{\mathrm{inc}}) = d_{s/m}\int\int \mathrm{d}E_{\mathrm{out}}\mathrm{d}\theta \frac{\chi(E_{\mathrm{inc}},E_{\mathrm{out}})}{\chi^m(E_{\mathrm{inc}},E_{\mathrm{out}})} \times \frac{a(E_{\mathrm{inc}},E_{\mathrm{out}},\theta)}{a^m(E_{\mathrm{inc}},E_{\mathrm{out}},\theta)}. \quad (6)$$

Note that $\epsilon_c(E_{\mathrm{out}},\theta)$, A_t and ϵ_γ from equation (4) dropped out, while ratios of PFNS and angular distributions between isotope of interest and monitor appear, thus reducing uncertainties associated with these terms. The difference in L_n between the monitor and isotope of interest is accounted for in the difference in PFNS, angular distribution, and the displacement of the monitor sample compared to the isotope of interest, $d_{s/m}$. This effect is often measured by performing and analyzing the monitor measurement with various positions of the sample, e.g., in references [19–23]. In the case of induced-fission measurements, fragment detection can depend on E_{inc} because of the momentum brought into the system.

3 Information needed for evaluations

Sufficient experimental data on $\overline{\nu}$, a short version encompassing both $\overline{\nu}_p$ and $\overline{\nu}_t$, are available for only a few isotopes, and only in restricted incident-neutron energy ranges, to evaluate $\overline{\nu}_p$ or $\overline{\nu}_t$ based exclusively on experimental data. A well-known evaluation that provides $\overline{\nu}_t$

values based on only experimental data is one of the thermal constants that is part of the Neutron Data Standard (NDS) project [10]. The thermal-constants effort is based on the work of Axton et al. [11]. Similar evaluation efforts were undertaken, e.g., [46,50], and all rely on a detailed analysis of experimental uncertainties including corrections of mean values and uncertainties. Nuclear data of $\overline{\nu}_p$ or $\overline{\nu}_t$ in the resolved resonance range are evaluated based on theory and available experimental data, e.g., undertaken as part of [49], but resonance data for $\overline{\nu}_p$ or $\overline{\nu}_t$ are not given for all isotopes. For instance, they are provided for ^{239}Pu $\overline{\nu}_p$ in ENDF/B-VIII.0 [57], but not for ^{238}Pu and $^{240-242}$Pu $\overline{\nu}_p$. The evaluations in the fast range can be based on a Bayesian analysis of differential experimental data (e.g., ^{239}Pu and ^{240}Pu $\overline{\nu}_p$ in ENDF/B-VIII.0), thus following fluctuations observed in the experimental data, or can be based on a simple linear fit to data (e.g., ^{241}Pu and ^{242}Pu $\overline{\nu}_p$ in ENDF/B-VIII.0). Approximating $\overline{\nu}_p$ by a linear function is based on the assumption that the fission yields and total-kinetic energy of the fission fragments do not vary with excitation energy and that the total energy released through fission γs follows a linear dependence [58]. However, measurements of the total kinetic energy and fission yields as a function of incident-neutron energy show an energy-dependent behavior, see, e.g., [59]. In line with these physics considerations, several ^{235,238}U and ^{239}Pu $\overline{\nu}$ measurements as a function of incident-neutron energy, e.g., [15,17–25,36,38,54], have shown that the experimental data cannot be described well by one linear function. In the absence of differential experimental data, evaluated data are also based on models with systematics of model parameters, as done, e.g., in reference [60].

The incident-neutron energy, E_{inc}, and either $\overline{\nu}_p$ or $\overline{\nu}_t$ are used as a bare-minimum input for the evaluation. If $\overline{\nu}_p$ is evaluated and the measurement is of $\overline{\nu}_t$, the evaluator needs to correct for the delayed component. If the data were measured in ratio to a monitor, it would be desirable if the ratio data were reported. Otherwise, the nuclear data of the monitor observable, often ^{252}Cf(sf) or ^{235}U(n,f) $\overline{\nu}$, or a reference should be provided. It would be desirable to explicitly state what PFNS was used either by reference or model parameters. Given the convolution of the PFNS with many other observables in the analysis of $\overline{\nu}_p$ measurements in equations (4) and (6), it is difficult to correct with a new PFNS. However, if one knows how close the used PFNS was to current nuclear data, one can estimate potential missing uncertainties due to limited knowledge of the PFNS at the time of the experiment. Partial uncertainties for all uncertainty sources listed in the templates should be provided, if applicable to a particular measurement. The $\overline{\nu}_p$ and $\overline{\nu}_t$ can be measured to high precision. However, even small variations in $\overline{\nu}$ of major actinides can impact the simulated neutron-multiplication factor, k_{eff}, of critical assemblies by a substantial amount. For instance, a change of 0.1% in a relevant energy range of ^{239}Pu(n,f) $\overline{\nu}_t$ can lead to a 100-pcm (i.e., a 0.1%) change in k_{eff} of a Pu assembly, where approximately 210 pcm is the difference between a controlled critical assembly and an accident emitting lethal radiation doses [61]. Hence, reporting complete and realistic uncertainties for $\overline{\nu}_p$ and $\overline{\nu}_t$ measurements is central for realistic application simulations and their bounds. Along the same lines, the experimental set-up (e.g., time the gate is open, size and isotopic composition of the neutron detector, through-tube size, neutron-producing reaction, impurity level), all pertinent corrections (e.g., background, foil thickness, angular distribution of fission fragments, dead-time, impurities, geometry, spurious structures in neutron flux, delayed γs, displacement of fission sample, false fissions, French effect) and analysis techniques should be documented in great detail, enabling the evaluator to judge the quality of the measurements and data reduction at a later time.

4 Template

A listing of all relevant uncertainty sources for $\overline{\nu}_p$ and $\overline{\nu}_t$ measurements is provided below, along with the proposed template values. All uncertainties here are given relative to $\overline{\nu}_p$ and $\overline{\nu}_t$ in percent (%) unless otherwise stated. Some uncertainty values seem very small, but one should consider that these measurements were built to reduce correction factors to a minimum and, hence, the associated uncertainties. Table 1 provides a template of uncertainties expected in absolute and ratio liquid-scintillator measurements, while Table 2 gives a template for Mn-bath measurements. Table 2 focuses mostly on uncertainties expected in measuring the neutron-count rate, c_n. Several different techniques were employed to measure the fission count rate, c_f, with differing uncertainty sources and values for each measurement type. Given that and the low number of ^{252}Cf(sf) $\overline{\nu}$ Mn-bath measurements, not enough statistics were available to give a template for specific uncertainty sources for c_f for each measurement type. Hence, the uncertainty sources entering δc_f were not split out in Table 2.

Counting-statistics uncertainties. No counting-statistic uncertainties, δc, are provided in both templates since these depend strongly on the measurement time, neutron flux (if applicable), detector response, etc., and are, thus, hard to estimate. We recommend rejecting a data set for evaluation purposes if this very basic uncertainty information cannot be, at least, roughly estimated (e.g., one-third of the total uncertainty), given that many $\overline{\nu}_p$ and $\overline{\nu}_t$ measurements are claimed to be of high precision. This high precision needs to be backed up by a reasonably informative uncertainty quantification.

Counting-statistics values depend strongly on the absolute measurement time, fission-detector response, and neutron flux for liquid-scintillator measurements. Hence, δc varies significantly across different measurements. For instance, δc values of 0.0012% to 3.9% can be found across ^{239}Pu(n,f) $\overline{\nu}$ measurements [12,14,19–23,26,35,38] and 0.08–0.8% can be found in EXFOR across ^{252}Cf(sf) $\overline{\nu}$ measurements [1,4,5,7–9,27,29,30]. The neutron-counting statistics uncertainty, δc_n, across various ^{252}Cf(sf) $\overline{\nu}$ Mn-bath measurements assume values from 0.1–0.2% [3,5,9,30,45], while the fission-counting uncertainty varies from 0.05–0.2% across references [5,7,30]. However, it

Table 1. Typical uncertainty sources encountered in absolute and ratio liquid-scintillator measurements of $\overline{\nu}_t$ are listed, along with realistic ranges of estimates that can be assumed if none are provided for a particular measurement. Also, off-diagonal correlation coefficients for each uncertainty source (for the same and different experiments) are roughly estimated. We implicitly assume that the typical tanks have high or similar detector efficiencies of ∼80% which is indeed often the case. The correlation functions are defined in reference [62].

Unc.	Absolute (%)	Ratio (%)	Cor(Exp$_i$)	Cor(Exp$_i$,Exp$_j$)
δc	Must be provided	Must be provided (δc & δc^m)	Diagonal	None
δc_{DG}	0.1	0.12	Full	Full
δb	0.15	0.5	Gaussian	0.2 for same n source 0 otherwise
δc_{ff}	–	0.22 (high α-activity sample)	Gaussian	0.2
	-	0.15 (low α-activity sample)		
δc_{FE}	0.1	–	Gaussian	0.2
$\delta\omega$	see Table 3	see Table 3	0.9	0.9 (same method & isot.) 0.1 (different isotope)
$\delta\tau$	0.1	0.08	Full	Low (∼0.2)
$\delta\varepsilon_\gamma + \delta\varepsilon_c$	0.2	N/A	Gaussian	Gaussian
$\delta\chi$	0.23	0.16	Gaussian	Full (same E_{inc})
		0.5 (2^{nd}-chance fission)		Gaussian (different E_{inc})
δL_n	0.2	N/A	Full	0.5
δa	N/A (isotropic)	0.01–0.3	0.8–1.0	0.6
		0.5 at 2^{nd} c.f. and >10 MeV		
$\delta\overline{\nu}^m$	N/A	From libraries/reference	Full	Full
δd	N/A (point source)	0.1–0.3	Full	0.8–0.9 (not corrected)
$\delta d_{s/m}$	N/A	0.05	Full	None
ΔE_{inc}	–	Estimate from similar facilities at the same E_{inc}	Full in E_{inc} space	0

holds that δc_n should be provided for a high-precision measurement. The correlation matrix associated with δc is usually diagonal for $\overline{\nu}_p$ and $\overline{\nu}_t$ measured within the same experiment, and not correlated to other measurements.

Delayed gamma-ray uncertainties. Delayed γs arise mainly as part of the decay of isomeric states with half-lives on the order of 70 µs for gates that are open less than 500 µs [63]. Some delayed γs from the β decay of the fission fragments of another fission event could also be measured, but to a lesser extent. These delayed γ rays are recorded in liquid-scintillator measurements along with those emitted after capturing prompt-fission neutrons in the scintillator material while the neutron-counting gate is open. This uncertainty source does not appear for Mn-bath measurements, as the γ rays emitted from the Mn solution are measured in a re-entrant well separated from the source.

The resulting delayed-γ background, c_{DG}, is corrected in absolute and ratio liquid-scintillator measurements by a combination of measurements and calculations of delayed γ-ray cascades [1,21–23,38,64]. For instance, a measurement with a low bias, i.e., low E_γ threshold, (including delayed γs) and a high bias (supposed to suppress most of the delayed γs) gave an estimate of c_{DG} for the experiment of Gwin et al. [21–23]. This measurement was counter-checked with simulations based on expected γ-ray cascades. Uncertainties, δc_{DG}, ranging from 0.1–0.2% were found for liquid-scintillator ratio data [21–23,38,64], with a median of 0.12% that is adopted for Table 1. δc_{DG} for absolute data was estimated to be 0.1% based on the assessment of these uncertainties for Boldeman, Asplund-Nilsson, and Hopkins data in reference [1]. A full correlation is assumed for δc_{DG} for the same and different experiments using the absolute and ratio liquid-scintillator technique, given that most likely the same decay data and assumptions for the simulation are used.

Random-background uncertainties. False-fission and delayed-γ background events are not part of the random-background correction, b, for liquid-scintillator measurements as these two corrections are treated separately.

Two different types of backgrounds are encountered in ratio liquid-scintillator measurements: (a) neutron-beam-related backgrounds and (b) delayed neutrons. Delayed neutrons can be corrected with nuclear data. Neutron-beam-related background counts can be detected in the neutron counter either with their initial, or slightly degraded, incident-neutron energy, or can thermalize and

Table 2. Typical uncertainty sources encountered in Mn-bath measurements of $\overline{\nu}_p$ and $\overline{\nu}_t$ are listed along with realistic ranges of estimates if none are provided for a particular measurement. Also, correlation coefficients for each uncertainty source between different experiments are roughly estimated. No correlation coefficient is given between uncertainties of the same experiment at different incident-neutron energies as Mn-bath measurements are usually undertaken at one incident-neutron energy (thermal) or for spontaneous fission. A medium-range correlation would correspond to correlation coefficients of 0.5–0.8, while "Low" corresponds to approximately 0.2.

Unc.	Unc. (%)	Cor(Exp_i,Exp_j)
	c_n	
δc_S	Must be provided	0
$\delta\frac{\sigma_\text{S}}{\sigma_\text{Mn}}$ & $\delta\frac{\sigma_\text{H}}{\sigma_\text{Mn}}$	0.29	Full
$\delta\frac{N_\text{H}}{N_\text{Mn}}$	0.05	Medium
$\delta(1+G\overline{r}s)$	0.09	Full
$\delta\varepsilon_\text{Mn}$	0.2	Medium
$\delta(1-L_n)$	0.02	Medium
$\delta(1-S)$	0.05	Full
$\delta(1-O)$	0.1	Full
Mn-bath impurities	0.1	0
	c_f	
δc_f	0.32	Medium
$\delta\tau$	0.05	Low
$\delta\omega$	See Table 3	See Table 1

lead to a random room background. Some neutron-producing reactions can lead to groups of secondary neutrons of lower energy than the anticipated one. Thus, these secondary neutrons induce fission of lower incident-neutron energy than assumed to be measured, biasing $\overline{\nu}$. All of these neutron beam-related backgrounds would not drop out in ratio measurements relative to ^{252}Cf(sf) $\overline{\nu}$, as the latter is measured without the beam.

The random, room-return, neutrons, and stray γs were often measured by opening a gate 200–250 µs after the main neutron-counting gate was closed, assuming that no more prompt-fission neutrons should be detected by then [15,17,19,20,34,36]. Also, measurements using random gates were employed to determine this part of b [21–23]. The number of thermalized neutrons was often reduced by adequate shielding and also by measurements with and without this shielding [34,36]. Background originating from secondary neutron groups in the beam was usually determined by measuring the energy of the neutron flux directly [15,16,39]. Uncertainties are reported for experiments described in references [12,16,21–23,34,35,38] spanning from 0.08–3.5%, with a median of 0.5% that is suggested as a value for δb if nothing else is known about the measurement. A Gaussian correlation is suggested for δb across the same experiment, given that b is often measured. Zero correlation is suggested for δb across experiments, unless the same neutron-beam type was used (common second-energy groups). In this case, a correlation of 0.2 is suggested.

The delayed and incident-beam neutrons can also lead to b for absolute liquid-scintillator experiments, which might be surprising as most of them are measuring spontaneously-fissioning sources. Even then, the neutron-detector efficiency is often measured with a neutron beam [2,15]. In these two experiments, a combination of shielding and filters reduced this background and measurements with random gates quantified b. The size of b is often reduced as a triple coincidence (fission fragments in the fission detector, prompt-fission γs in the scintillator, and fission neutrons in a proton-recoil detector) is used to open the gate. In addition to these above-mentioned contributions to b, the proton-recoil background may need to be quantified [1]. Asplund-Nilsson et al. addressed this background by pulse-shape discrimination [27]. Uncertainties of 0.1–0.2% are mentioned in reference [1], where we adopt the mean due to lack of statistics.

No b needs to be corrected for Mn-bath measurements of ^{252}Cf(sf) $\overline{\nu}_t$, as no neutron beam is used for these measurements. However, if this technique is used for neutron-induced measurements of $\overline{\nu}_t$, uncertainties due to incident-beam neutrons should be considered.

False-fission uncertainties. False-fission uncertainties, δc_{ff}, are related to a random-coincidence background in ratio and absolute liquid-scintillator measurements that leads to an incorrect opening of the neutron-counting gate. As no gate is opened in Mn-bath measurements, this uncertainty source does not apply.

The background counts, c_{ff}, originate from the following effect: the fission detector is fired by α particles or noise and thus opens the neutron-counting gate[2]. The neutron detector then registers background neutrons [21–23,64] assuming they are fission neutrons. This effect is usually measured and calculated. For instance, Gwin et al. [21–23] introduced a mock α pulse into the electronics of their experiment and measured the resulting background neutrons that can then be subtracted from all measured counts. However, one needs to know how often α particles are likely to fire the fission detector compared to the rate of fission. This rate of false-fission events compared to fission ones is usually estimated from the α activity of the sample. The resulting background-count rates can be counter-checked with a beam-off measurement [21–23,64].

The associated uncertainty, δc_{ff}, is larger at low E_inc, as more false-fission events are registered relative to real ones [21–23]. Uncertainties are given for data of references [16,21–23,35,38] range from 0–0.5% with a relatively high median of 0.22% that is adopted here for samples with high α activity (^{239}Pu), while a value of 0.15% is adopted for lower-activity samples (^{235,238}U).

[2] Some α-particles can usually by discriminated from fission events on the signal amplitude by putting a threshold on the device. However, α pile-up of highly radioactive samples (e.g., ^{239}Pu) can pose an issue as the α-signal amplitude (not the shape) becomes similar to that of fission fragments. Then, a background measurement with the sample in place but without the beam can help identify the rate of false-fission events as mentioned below.

A medium-range uncertainty with Gaussian correlation is given as part of c_{ff} corrections are measured and the associated uncertainties are random background-counting uncertainties. Some measurements take recourse to nuclear data and assumptions on the α-activity of the sample to estimate the relative frequency of gates opened by αs from the sample; then a Gaussian correlation is also adequate. These assumptions affect equally all $E_{\rm inc}$ measured with the same sample. Correlations between δc_{ff} of different measurements are assumed to be weak (with correlation coefficient 0.2), given that the only assumption common to both measurements, and thus introducing non-zero correlations, would be the α activity of the isotope in question.

In absolute liquid-scintillator ^{252}Cf(sf) $\overline{\nu}$ measurements, c_{ff} is usually negligible because a coincidence between the fission detector and prompt-fission γ rays being detected in the scintillator was required to open the gate [2,8,15]. However, as they also used proton-recoil measurements to open the gate at the same time, this introduced the French effect into their results, which does not appear for ratio liquid-scintillator measurements.

French effect uncertainties. The French effect, found by Soleihac and first reported at the IAEA Consultants meeting held at Studsvik, Sweden, in June 1970 [65], $c_{\rm FE}$, only affects absolute liquid-scintillator measurements, as it originates from using a coincidence of several signals to open the neutron-counting gate. The bias results from a dependence on registering fission fragments in the fission chamber, scintillator pulses from prompt-fission γs, and proton recoils on the number of neutrons detected per gate [65]. The physics mechanism behind this effect is not fully understood and the magnitude depends on the set-up and so can be difficult to estimate retrospectively, but for new measurements can be experimentally assessed. It affects the measurements of [1,2,8,15,27]. Reported uncertainties in the associated literature, EXFOR, and in references [1,46] cite uncertainties from 0.1–0.48%. The effect is measured and depends strongly on the set-up used. Boldeman states in reference [1] that this effect is usually small (except for the data of Ref. [27]), hence, a small uncertainty of 0.1% is recommended with a Gaussian correlation and low correlation between experiments.

Impurity uncertainties. Sample-impurity uncertainties, $\delta\omega$, apply to all measurement types. $\delta\omega$ can be effectively controlled by employing high-purity samples such as for instance used in [12,21–23,34,38] (they utilized ^{239}Pu samples with purity close to or larger than 99.9%). Spontaneously fissioning contaminants and their contribution to $\overline{\nu}_p$ and $\overline{\nu}_t$ were determined in incident-neutron energy-dependent $\overline{\nu}$ measurements [21–23,35] with a beam-off measurement. Non-spontaneously fissioning contaminants can be measured (e.g., by mass-spectroscopy [66]) and their contribution to $\overline{\nu}$ can then be corrected by using nuclear data [17,21–23,38]. The value of $\delta\omega$ depends thus on the accuracy of the contamination measurement, the level of impurity, and the nuclear data used. For ^{239}Pu(n,f) $\overline{\nu}$, $\delta\omega$ values between 0.03 and 0.1% can be found [17,21–23,35] with some experiments giving even lower values of 0.001% [12,38]. $\delta\omega$ values spanning from 0.02–0.1% can be found for ^{252}Cf(sf) $\overline{\nu}$ measurements. Also, EXFOR files were searched for ^{232}Th, ^{237}Np, ^{233,235,238}U, ^{240,241}Pu, and ^{241}Am $\overline{\nu}_p$ to obtain recommended values of $\delta\omega$ per isotope in Table 3. Unfortunately, $\delta\omega$ values were found for only a few isotopes. Due to the scarce statistics (i.e., a small number of documented cases), only a value of $\delta\omega$ could be given per isotope, not depending on impurity level or incident-neutron energy. Both factors play a role: for instance, a ^{238}U impurity in a ^{235}U sample could bias $\overline{\nu}$ in the fast range, but is negligible below the fission threshold of ^{238}U. Also, as said above, $\delta\omega$ can be driven to be negligible by using very pure samples. The issue of isotopic impurity is an important one for samples that are not highly enriched, which could be the case in the earliest measurements of $\overline{\nu}$. The $\delta\omega$ values in Table 3 are recommended to be used if no information is given on the impurity levels in the sample. Like all other uncertainty values, $\delta\omega$ is understood to be given relative to $\overline{\nu}$.

Table 3. Recommended values for $\delta\omega$ in $\overline{\nu}_p$ and $\overline{\nu}_t$ are listed as found in EXFOR for various isotopes from thermal to 20 MeV and various degrees of impurities. The median of all $\delta\omega$ values found for one isotope is given as the recommended value.

Isotope	$\delta\omega$ (%)
^{233}U	0.05
^{235}U	0.05
^{239}Pu	0.07
^{241}Pu	0.1
^{252}Cf	0.1

It is interesting to note that the largest median value of $\delta\omega$ appears for ^{252}Cf(sf) $\overline{\nu}$ despite it being the standard. The reason for this finding might be due to considerable alpha pile-up in the impurity-level determination. Also, a significant ^{250}Cf component is inevitable with fresh sources having a mass fraction of ca. 10/85 compared to ^{252}Cf(sf) which increases with age and becomes prohibitively large for samples older than roughly 15 years [67]. For fresh sources, the $\delta\omega$ related to the ^{250}Cf content should be small.

It should also be mentioned that some small adjustments to older data might be used as $\overline{\nu}$ and half-lives of the impurities might be different enough to impact the estimate of ω correction factors. It is expected that this does not apply to ^{252}Cf sample as the spontaneous-fission branching ratio is very high.

A larger correlation coefficient is assumed for correlations between $\delta\omega$ of the same experiment as usually the same sample is used at all $E_{\rm inc}$ and nuclear data used for the correction is strongly correlated. If the same method was employed across different experiments and the same isotope was measured, a strong correlation can be assumed. If a different isotope was measured, the correlation is low because different nuclear data were used for the correction of impurities in the sample.

Dead-time uncertainties. Dead-time uncertainties, $\delta\tau$, apply to all measurement types. When neutron pulses pile up during the experiment, the system is dead to measuring other neutron events. Similarly, when α particles pile up, the fission-detection system (for c_f in Mn-bath measurements and for opening the gate in liquid-scintillator measurements) can be dead. The $\overline{\nu}_p$ and $\overline{\nu}_t$ need to be corrected for this dead-time effect. Descriptions of numerical correction procedures can be found in references [17,21–23,36,38], while it was minimized in reference [36] by carefully selecting detectors and shielding to reduce dead time induced by background counts. For ratio measurements, the dead-time uncertainty reduces to the ratio of dead-time for the isotope of interest and the monitor sample. Related dead-time uncertainties in ratio liquid-scintillator measurements, $\delta\tau$, for $\overline{\nu}$ span values of 0.02–0.5% with a median of 0.08% that is recommended in Table 1. A median of 0.1% is found for absolute liquid-scintillator measurements, while a total $\delta\tau$ (for fission and neutron counting) of 0.05% is given for Mn-bath measurements.

This uncertainty source would be strongly correlated for the same experiment as functional forms are used for correcting τ while a weak correlation is assumed between measurements due to reliance on different equipment and different background-reduction techniques.

Uncertainty in detecting capture-γ rays. The uncertainty in the detection of γ rays resulting from neutron-capture in the scintillator, $\delta\varepsilon_\gamma$, are considered in $\delta\varepsilon_c$ as these two uncertainties are usually given in a combined manner. The reason for this is that usually ε_γ is determined by measuring ε_n at a specific E_{inc} and angle. ε_γ is then extracted by knowing ε_c and L_n from MC simulations and having a defined anisotropy introduced by the through-tube, A_t. Hence, there is a strong correlation between $\delta\varepsilon_\gamma$ and $\delta\varepsilon_c$. ε_γ only appears for absolute liquid-scintillator measurements and drops out in ratio measurements.

Uncertainty of neutron-capture efficiency. The uncertainty related to the neutron-capture efficiency of the Gd or Cd-loaded scintillator material, $\delta\varepsilon_c$, only appears for absolute liquid-scintillator measurements while ε_c cancels in ratio measurements in equation (6). The term ε_c is often calculated with neutron-transport codes. To this end, the codes rely on nuclear data of the capturing material (e.g., hydrogen, gadolinium, cadmium) dependent on, both, energy and angle [1,15]. ε_c can also be measured in combination with ε_γ [2,15,27]. Even if ε_c is determined by simulations, usually validation measurements are performed [1,15]. The neutron-detection efficiency is then measured at a specific E_{inc} and angle. However, one still needs MC simulations for L_n and nuclear data for χ and a to obtain ε_n [2,15,27].

Uncertainties of 0.1–0.2% are reported for the data of Boldeman and Asplund-Nilsson et al. in reference [1], while 0.388% is given in the EXFOR entry of [8]. Again, the median of 0.2% is assumed which applies to the combination of $\delta\varepsilon_c$ and $\delta\varepsilon_\gamma$. A Gaussian correlation is assumed as both measurements and nuclear data are used for determining $\varepsilon_c\varepsilon_\gamma$.

PFNS uncertainty. The PFNS, χ, enters as an important factor in the analysis of each measurement technique presented here. It enters in equations (4) and (6) for absolute and ratio liquid-scintillator. χ does not appear explicitly in equation (2). However, it has to be considered implicitly when simulating the terms $(1-L_n)$ (neutrons leaked), $(1-S)$ (neutrons recaptured by material in the cavity) and $(1-O)$ (neutrons lost by charged-particle reactions with oxygen or sulfur) via neutron-transport codes as one needs to know the energy distribution of neutrons being released as part of the fission process. To this end, representative values need to be selected for χ, either from nuclear-data libraries or by assuming model-parameter values (e.g., Maxwellian temperature or Watt parameter values) entering a functional form. However, given the convoluted nature of χ with other observables to yield ε_n or $(1-L_n)(1-S)(1-O)$ in equation (2), it is neither straight-forward to correct with more recent χ values nor to estimate $\delta\chi$ based on our present-day understanding of χ. One would need to know all factors entering equations (4), (6), and $(1-L_n)(1-S)(1-O)$. In addition, the absolute value of $\delta\chi$ depends not only on how well the chosen numerical values for χ reproduce actual physics properties, but also on other factors appearing in equations (4), (6), and (2). For instance, if one employs a highly efficient neutron detector, $\delta\chi$ relative to $\overline{\nu}$ will be smaller than a less efficient one for the same values of χ.

In absolute $\overline{\nu}_p$ and $\overline{\nu}_t$ measurements, χ enters absolutely as well, while the ratio of χ of the isotope of interest and the monitor isotope is considered in ratio measurements. Quantifying only the difference between two prompt-fission neutron spectra leads usually to smaller $\delta\chi$ than if χ has to be given absolutely. Consequently, $\delta\chi$ values of absolute ^{252}Cf(sf) $\overline{\nu}$ liquid-scintillator measurements are overall larger than those found for ratio measurements of ^{239}Pu(n,f) $\overline{\nu}_p$; $\delta\chi$s found for the ^{252}Cf(sf) $\overline{\nu}$ data of [1,2,8,27,29] assume values in the range of 0.04–0.5% with a median of 0.23% that is used for the template for absolute liquid-scintillator measurements. Values ranging from 0.01–1% are found across several ^{239}Pu(n,f) $\overline{\nu}_p$ measurements [12,16,17,19–23,26,38] with a median of 0.16%. An additional complication with the PFNS of ratio measurements poses the incident-neutron energy dependence of χ. If the monitor value is measured at one defined incident-neutron energy, as is the case for using the monitor ^{252}Cf(sf) $\overline{\nu}$ ($E_{\text{inc}}=0$ as spontaneously fissioning), the overall size of the difference between χ of isotope of interest and monitor depends on E_{inc}. The χ of an isotope of interest usually differs from the χ of ^{252}Cf(sf). Even greater differences are expected for neutron-induced fission near the second-chance-fission threshold. At these E_{inc}, distinct structures can be observed in χ for E_{out} around a few hundred keV across many isotopes, see e.g., references [53,68–71]. While χ also hardens with E_{inc} for the isotope of interest, the mean energy might actually be closer to that of the χ of ^{252}Cf(sf) reducing the difference between the two χ which is counter-balanced by structures such as $\geq 2^{\text{nd}}$-chance fission and the pre-equilibrium component for the χ of interest. Hence, the median of 0.16% is suggested for ratio liquid-scintillator measurements in Table 1 for all E_{inc} except for the second-chance-fission

threshold, where 0.5% is suggested. It should be mentioned that these values are isotope-dependent. Some isotopes, e.g., ^{238}U, show larger second-chance fission structures than others leading to increased $\delta\chi$ for the same neutron-detection efficiency. No $\delta\chi$ is given in Table 2 for Mn-bath measurements given the convoluted nature of χ with the term $(1-L_n)(1-S)(1-O)$. Instead, uncertainties are provided for the individual terms—$(1-L_n)$, $(1-S)$, and $(1-O)$—which contain $\delta\chi$.

If the same values for χ/χ^ms are used for one (liquid-scintillator) experiment, $\delta\chi$ is fully correlated. If an energy-dependent χ/χ^m is used, a Gaussian correlation is recommended. The reasoning behind this choice is that evaluations of χ are usually based on models leading to strong correlations between χ at different $E_{\rm inc}$. If the same or similar assumptions on χ are made across different experiments at the same $E_{\rm inc}$, $\delta\chi$ is fully correlated across these experiments. If the same χ is chosen across experiments at different $E_{\rm inc}$, a Gaussian correlation would be recommended in line with the discussion above. It would be best practice for experimental results to be reported along with sufficient detail to allow the PFNS uncertainty to be re-calculated at a later time or when a new evaluation of χ becomes available.

Neutron-leakage uncertainty. The leakage of neutrons, L_n, out of the through-tube of liquid-scintillator measurements is convoluted in equation (4) with the PFNS, χ, the angular distribution of prompt-fission neutrons, a, and the geometrical anisotropy of the experimental configuration A_t. All these factors, χ, a, and A_t enter in MC simulations of L_n [1] that in turn enter the determination of ε_n. In ratio measurements, the geometrical anisotropy for monitor and isotope of interest should be nearly the same except for the effect of the displacement of the sample with uncertainties considered in $\delta d_{s/m}$. The difference in neutron leakage can be traced back to the difference in χ and a for the monitor and isotope in question. Hence, L_n does not appear in equation (6) and δL_n is not applicable.

δL_n is also given rarely for absolute-liquid scintillator measurements as it is either considered in δA_t as in reference [2] or in the neutron-detector efficiency [15]. In a review by Boldeman [1] a value of 0.2% was given for his own ^{252}Cf(sf) $\overline{\nu}_p$ measurement and 0.3% for the measurement of Asplund-Nilsson [27], while in the original publication, no δL_n is reported separately and L_n is discussed as part of $\delta\varepsilon_n$. A value of 0.2% is recommended for absolute liquid-scintillator measurements for the sake of completeness if not considered as part of other uncertainty sources. A full correlation is assumed for δL_n of the same experiment as L_n is usually calculated with MC codes relying on geometrical assumptions and nuclear data, while a strong correlation factor of 0.5 is assumed between experiments.

The leakage of neutrons out of the Mn bath, $(1-L_n)$, is considered explicitly in equation (2), and associated uncertainties, $\delta(1-L_n)$, ranging from 0.01–0.04% (about 10% of the correction factor itself) are provided by references [3,5,6,30,45] with a more recent MC study [47] confirming simulated uncertainties as low as 0.01%. We recommend a slightly larger median value of 0.02% (still negligibly small) which reflects the fact that most measurements were undertaken decades ago where neutron-transport or diffusion calculations were less accurate and precise than today's counterparts [3,45]. These simulations rely on assuming a χ of the source as well as knowing the concentration of the Mn-bath solution, geometry of the set-up itself, and shielding [3]. $(1-L_n)$ can also be measured [5,30,45], e.g., by using two baths of varying size. Given that $\delta(1-L_n)$ relies on very similar nuclear data to be calculated but also assumptions that are unique to an experiment campaign (geometry) and explicit measurements [45], a medium-range correlation is assumed between $\delta(1-L_n)$ of different experiments.

Uncertainty of angular distribution of fission neutrons. A correction for the angular distribution of fission neutrons, a, is needed for $\overline{\nu}$ measurements in the fast range. As measurements in the fast range are usually undertaken with the liquid-scintillator technique, a appears here for these types of measurements. The incident-neutron energy beam leads to a preferred direction of the fission fragments with respect to the angle of incident neutrons, see e.g., [66], because of (a) the forward boost of fission fragments that becomes significant for $E_{\rm inc} > 10$ MeV, and (b) the inherent anisotropy of fission fragments. The outgoing prompt-fission neutrons tend to be emitted into the direction of the moving fragments in the reference system of the laboratory [38] leading to a non-negligible angular dependence of fission neutrons. The resulting angular distribution of prompt-fission neutrons is both dependent on the incident-neutron energy and the isotope [72]. At thermal, the prompt-fission neutrons can be assumed to be emitted isotropically on average, while an angular distribution of fission neutrons becomes noticeable for incident-neutron energies as low as 1 MeV for ^{235,238}U and ^{239}Pu [72] and is isotropic only below approximately 200 keV. For spontaneous fission, the fission fragments are emitted isotropically and so are the neutrons. Hence, this effect does not appear if all of the fissions of ^{252}Cf are detected. If only some part of the angular range of the fragments of ^{252}Cf(sf) is detected, as it will be for any fragment detector, then the associated neutrons will not be isotropic, but the effect will be less pronounced compared to neutron-induced fission in the fast range. Due to the same reasoning, a/a^m does not cancel in ratio measurements where the isotope of interest is measured relative to ^{252}Cf(sf) $\overline{\nu}$.

The correction for this effect is usually calculated by taking into account the geometry of the experiment (especially the through-tube) and assuming an angular distribution of fission fragments [17,21–23,38,66]. It is strongly intertwined with the neutron-leakage, L_n, and asymmetry of the measurement configuration, A_t. If the neutron detector fully enclosed the fission detector (i.e., a 4π environment), no correction for a would apply. However, the through-tube is needed for housing the detector and giving way to the neutron beam. This reduces the geometry to be less than 4π. δa is one of the least understood uncertainty sources for $\overline{\nu}$, given that the angular distribution of fission neutrons is not very well-known today and even less so in the mid-60s to 80s, when many $\overline{\nu}$ measurements were

performed. Uncertainty values related to the angular distribution of fission neutrons, δa, range for ^{239}Pu(n,f) $\overline{\nu}$ measurements from 0.002–0.3% [12,16,17,21–23,35,36,38]. The lowest uncertainties (0.002–0.1%) are reported for data below 2 MeV [12,17,35,38], while values of approximately 0.3% are reported for data at higher $E_{\rm inc}$ [21–23,36]. Exceptions are data of [38,54] that have low δa values despite being measured to $E_{\rm inc} > 2$ MeV, where the contribution of a is non-negligible [72]. In the template, 0.1% is proposed for δa from 0.2 up to 1 MeV going up to 0.3% above 2 MeV and 0.5% at the second-chance-fission threshold and at $E_{\rm inc} > 10$ MeV. δa is assumed to be zero for $E_{\rm inc} < 0.2$ MeV. At the second-chance-fission threshold, the angular distribution of FF is very large in general, leading to a larger a. Also, the forward boost of fission fragments induced by incident neutrons should be considered for $E_{\rm inc} > 10$ MeV, leading to overall larger uncertainties in this energy range. It should be stressed that δa and a are not well understood and both values should be carefully examined within new experiments.

Off-diagonal correlation coefficients between 0.8–0.9 are assumed between δas at different $E_{\rm inc}$ for the same experiment, as nuclear data and functional relationships are usually used for corrections. A correlation of 0.6 is assumed between different experiments, as the same functional relationships would have been used and similar nuclear data, but the accuracy of geometrical considerations differs between measurements. Zero uncertainty is assumed for absolute measurements that are usually taken of spontaneously fissioning systems, where a related to the detector is not applicable.

Asymmetry uncertainty. The asymmetry uncertainty, δA_t, only occurs for absolute liquid-scintillator measurements and has to be considered for a correct calculation of neutron leakage. For only one ^{252}Cf(sf) $\overline{\nu}$ measurement, i.e., [2], a separate uncertainty is given for δA_t of 0.03%. Otherwise, δA_t is part of either δL_n or δa. Hence, we do not have an entry for δA_t in Table 1, considering it part of δL_n or δa. δA_t drops out in ratio liquid-scintillator measurements, as the same asymmetry applies to the isotope of interest and monitor measurements. Any difference in δA_t stemming from the variability in the location of the sample of interest and the monitor one is considered in $\delta d_{s/m}$. It can be estimated experimentally by shifting the sample.

Monitor uncertainty. The monitor uncertainty, $\delta\overline{\nu}^m$, is usually straightforward to estimate if one knows what data were used for $\overline{\nu}^m$ in equation (6) or if ratio data are explicitly provided. The latter case is preferred, as it gives evaluators the possibility to use the currently best available nuclear data for $\overline{\nu}^m$. Usually, ^{252}Cf(sf) $\overline{\nu}_t$ is used as monitor. The current value recommended by the NDS project is 3.7637 ± 0.42 % [10]. This uncertainty only applies to ratio measurements.

If the same monitor applies to all data across incident-neutron energies, as is the case for measurements relative to ^{252}Cf(sf) $\overline{\nu}_t$, this would lead to a fully correlated $\delta\overline{\nu}^m$ across one experiment. The same nuclear data should be used to represent the same a monitor observable throughout an evaluation, leading to a full correlation of $\delta\overline{\nu}^m$ across all experiments measured relative to the same monitor observable.

Uncertainty due to thickness of sample. The uncertainty due to the thickness of the sample, δd, only appears for measurements that do not employ a point-source sample. Usually, small and thin samples are used for ^{252}Cf measurements. Hence, a template value is only given for ratio measurements. This correction factor applies because fission fragments do not leave the thick foil or lose too much of their kinetic energy before escaping the foil. Thus, they fail to trigger the fission detector that opens the gate to measure neutrons. The size of d depends on the thickness of the sample, but also on how the sample was manufactured. If the sample material is sprayed or evaporated onto a foil, the resulting samples are usually the most uniform ones. Thus fewer fission fragments are lost than when a sample of the same average thickness is electroplated or, in the worst case, rolled or painted. This effect can be counter-balanced by a fission detector with good efficiency that is also able to register fission fragments of low kinetic energy.

This effect is discussed in great detail in references [21–23,56], where reference [56] provides a brief overview on previous work. Correction factors for different thicknesses were obtained in reference [56] by measuring a ^{252}Cf point source with increasing layers of lead. The results show that d is linear up to a thickness of 2500 μg/cm^2 (correction factors are provided in Table I of this reference). Gwin [21–23] measured $\overline{\nu}$ with two samples of different thicknesses and simulated the effect. These investigations led to an uncertainty of 0.05%, which is a lower bound, as Gwin employed a thin sample (100 μg/cm^2), thus minimizing the effect of d. An uncertainty of 0.1% is assumed for a high fission-detection efficiency and a sample thicker than that of Gwin. δd can rise to 0.3% for thick samples (700 μg/cm^2).

A full correlation matrix is assumed for δd of each individual experiment as d is a multiplicative correction factor unless samples of different thicknesses were employed at different $E_{\rm inc}$. It is assumed to be strongly correlated across different measurements, given that this effect was not frequently corrected. However, if an independent measurement was undertaken for an individual experimental effort, no correlation should apply.

Sample-displacement uncertainty. The uncertainty due to the displacement of the sample, $\delta d_{s/m}$, appears only for ratio measurements, because it accounts for possible biases introduced in the measured quantity by small deviations between the position of isotope of interest and monitor samples. This displacement would lead to a difference in the neutron leakage between the sample and monitor, and thus lead to a bias in $\overline{\nu}$. The possible bias was quantified in references [12,21–23,38] for ^{239}Pu(n,f) $\overline{\nu}$ with very low uncertainty values $\delta d_{s/m}$ of 0.01–0.05% uncertainties. Gwin et al. [21–23] obtained these values by first determining a possible bias by measuring the ^{252}Cf sample in different positions in the through-tube. The authors then

assumed one-third to one-fifth of the measured correction as uncertainty. The upper bound of 0.05% is adopted for the template as a conservative estimate if this uncertainty source was not quantified.

As $d_{s/m}$ is an energy-independent multiplicative correction factor, a full correlation is assumed for $\delta d_{s/m}$ across data of the same experiment. A zero correlation between $\delta d_{s/m}$ of different experiments is assumed, as a displacement of the sample would be random between these experiments, thus leading to an independent bias across measurements.

Energy uncertainty. The incident-neutron energy uncertainty, δE_{inc}, or resolution, ΔE_{inc}, depends on the neutron source which can be a white or mono-energetic neutron source. For TOF measurements, it depends on the TOF-path length, energy, and uncertainty in resolving the exact timing of the fission pulse, while secondary-neutron groups can lead to a smearing of E_{inc} in mono-energetic measurements. Given that, it would be best to estimate δE_{inc}, if missing, based on existing uncertainty values from the same or similar facilities at the same E_{inc} rather than assuming one blanket value. To support this statement, it should be mentioned that δE_{inc} ranging from 0.034% to 27.5% are reported across [12–26,34–38].

A full correlation is assumed for the δE_{inc} of the same measurement in energy space, while no correlation is assumed between measurements, as the defining factors for uncertainties vary randomly between measurements.

Uncertainties stemming from those of thermalized hydrogen and sulfur cross sections as ratios to manganese. The fraction of neutrons captured by Mn in the Mn-baths depends on the ratio of cross sections of neutron-capture in Mn relative to that of those captured in hydrogen and sulfur at thermal energies, $\frac{\sigma_{\mathrm{H}}}{\sigma_{\mathrm{Mn}}}$ and $\frac{\sigma_{\mathrm{S}}}{\sigma_{\mathrm{Mn}}}$, respectively. These cross-section are usually represented by nuclear data and their uncertainties, $\delta\frac{\sigma_{\mathrm{S}}}{\sigma_{\mathrm{Mn}}}$ and $\delta\frac{\sigma_{\mathrm{H}}}{\sigma_{\mathrm{Mn}}}$, are propagated to uncertainties in $\overline{\nu}$ [3,5]. The ratio can also be determined by varying the concentration of, e.g., hydrogen ($N_{\mathrm{H}}/N_{\mathrm{Mn}}$) in the solution [30,45]. $\delta\frac{\sigma_{\mathrm{S}}}{\sigma_{\mathrm{Mn}}}$ and $\delta\frac{\sigma_{\mathrm{H}}}{\sigma_{\mathrm{Mn}}}$ are usually reported in a combined manner (both contain σ_{Mn}), with uncertainties range from 0.2–0.29% [3,5,30,45], where the by far dominant part stems from $\delta\frac{\sigma_{\mathrm{H}}}{\sigma_{\mathrm{Mn}}}$ [45]. Hence, additional measurements with varying $\frac{N_{\mathrm{H}}}{N_{\mathrm{Mn}}}$ were performed to determine $\frac{\sigma_{\mathrm{H}}}{\sigma_{\mathrm{Mn}}}$ [45]. A full correlation is assumed between $\delta\frac{\sigma_{\mathrm{S}}}{\sigma_{\mathrm{Mn}}}$ and $\delta\frac{\sigma_{\mathrm{H}}}{\sigma_{\mathrm{Mn}}}$ of different experiments, given that usually the same or similar nuclear data were employed. This uncertainty source naturally only applies to Mn-bath measurements.

Uncertainties due to number of hydrogen versus manganese atoms. The uncertainties in the ratio of the number of hydrogen vs Mn atoms, $\delta\frac{N_{\mathrm{H}}}{N_{\mathrm{Mn}}}$, can be determined very precisely by various methods (volumetric, gravimetric, and solution-density determination) [3,45]. It is rarely reported and Axton states in his review of Mn-bath measurements [45] that it is negligibly small, with a reproducibility uncertainty of 0.05% which is adopted in Table 2. A medium-range correlation is recommended between $\delta\frac{N_{\mathrm{H}}}{N_{\mathrm{Mn}}}$ of different experiments, given that similar methods are used to determine $\frac{N_{\mathrm{H}}}{N_{\mathrm{Mn}}}$ across experiments.

Uncertainties due to resonance capture of neutrons in manganese. The uncertainties in the resonance-capture term of neutrons in Mn, $\delta(1+G\overline{r}s)$, are usually given in a combined manner, given that all three parameters are used to derive the effective cross-section. This factor is either obtained by theoretical or MC calculations, depending on the Mn-activation integral and nuclear data [5,30,45]. Values for $\delta(1+G\overline{r}s)$ of 0.05–0.1% are reported for references [5,30,45] and the median of 0.09% is adopted in Table 2. Given that usually recourse to the same assumptions and data are taken, a full correlation is assumed between $\delta(1+G\overline{r}s)$ of different experiments. This uncertainty source naturally only applies to Mn-bath measurements.

Mn-bath efficiency uncertainties. Calibrating the Mn bath is usually undertaken with respect to well-known (standard) sources and by cross-comparison of various baths and sources in the international community [3,7,30,45]. Axton highlights in reference [45] that the efficiency, $\varepsilon_{\mathrm{Mn}}$, derived from this calibration will deteriorate invariably over time and recommends repetition of calibrations.

The associated uncertainty, $\delta\varepsilon_{\mathrm{Mn}}$, is a major uncertainty source for Mn-bath measurements of $\overline{\nu}$, with values ranging from 0.11–0.3% across [3,5,6,30,45], where the median, 0.2%, is recommended for the template. Medium-sized correlations are suggested for $\delta\varepsilon_{\mathrm{Mn}}$ between different measurements, given that common standards are used as well as cross-comparisons are undertaken across experiments.

Uncertainties due to neutrons captured by cavity material. In Mn-bath measurements, one has to account for neutrons lost as they enter the sample cavity or shell which creates the air space at the center of the solution and are recaptured by either the source or materials present in the cavity. The associated term, $(1-S)$ in equation (2), is usually simulated by MC neutron-transport or diffusion codes, taking into account the concentration of the Mn solution, the PFNS, χ, the geometry of the Mn bath, and diameter, thickness, and materials in the cavity [3,30,45,47]. The flux that is then calculated at the cavity boundary can be validated by measurements of this flux using various foils in the cavity. For instance, gold foils were used in references [5,45].

Associated uncertainties, $\delta(1-S)$, ranging from 0.03–0.1% were found for [3,5,6,30,45], with recent work reaching uncertainties as low as 0.05%. The median, 0.05%, of these uncertainties is adopted in Table 2. A full correlation is assumed between $\delta(1-S)$ of different experiments, given that corrections are usually calculated taking recourse to the same or similar nuclear data and χ.

Uncertainties due to neutrons captured by oxygen and sulfur. Fast neutrons are captured in Mn baths by oxygen and sulfur in (n,α) and (n,p) reactions. The associated term, $(1-O)$, in equation (2) is usually simulated with MC codes that track the position of neutrons from the source leading to (n,α) and (n,p) reactions [3,5,30,45,47]. To this end, one needs to know the outgoing-neutron energy distribution of prompt neutrons, χ, the concentration of the bath and the geometry of the set-up [45,47]. Validating experiments can be performed using known sources as described in references [7,45].

Associated uncertainties $\delta(1-O)$ of 0.06–0.1% are found across references [3,5,6,30,45], with a median of 0.1% that is recommended in Table 2. A recent report [47] obtained a value of 0.07% using modern codes and nuclear data. Also, a recent study by [73] showed that newly evaluated data (e.g., ENDF/B-VII.1 cross sections which are 30–50% lower than those of ENDF/B-VIII.0) can have a non-negligible impact, for instance, on the ^{252}Cf(sf) $\overline{\nu}_t$ data of Spiegel et al. A full correlation is assumed for $\delta(1-O)$ between different experiments, as the underlying simulations usually depend on the same nuclear data and a similar χ.

Mn-bath impurity uncertainties. Impurities in the Mn-bath solution can lead to thermalized neutrons being captured in additional reactions than discussed above [5,45]. The associated uncertainty depends on the isotopic composition and abundance of the impurities. Aleksandrov et al. estimated that 0.1% of c_n are recorded from events where neutrons are captured by impurities and gave this as a bounding uncertainty. This value is adopted in Table 2 and coincides with the uncertainty reported for [6]. It should be mentioned that this uncertainty estimate is highly dependent on the actual contamination level in the bath, and, hence, this uncertainty should only be used if no other information can be derived from other sources. One should be able to study this effect by gamma spectroscopy and half-life studies as well as losses due to competitive capture compared to Mn. Zero correlation is assumed for Mn-bath impurity uncertainties of different experiments, as two distinct baths are expected to have different impurities necessitating dissimilar corrections.

Fission-rate uncertainties. The fission-rate uncertainties, δc_f, encompass several uncertainty sources appearing for measuring the fission rate, c_f. As mentioned above, several techniques were employed to determine c_f in various ^{252}Cf(sf) $\overline{\nu}$ measurements: solid-angle counting of fission fragments using Si-surface barrier detectors [9,30], fission-fission coincidence counting [3] or neutron-fission coincidence counting [7]. We have for each measurement type too few individual measurements available to reasonably split out uncertainty sources and generate a template for each of those measurement techniques. If one compares combined uncertainties of δc_f across the measurements of [3,5–7,9,30], one ends up with a median value of 0.32%, which is recommended in Table 2. This value should be seen as a guide to compare if given total uncertainties related to δc_f are realistic, and as a rough estimate if nothing else is given. However, this is a major uncertainty source, and if it is not provided for a particular data set, we would recommend not to include the data in the evaluation, unless there are no other measurements of the observable available. Usually, δc_f contains counting statistics uncertainties (0.05–0.2% [5,7,30]), solid-angle uncertainties (0.05–0.6% [5,7,30]), back-scattering from sample (0.1–0.5% [6,30]), self-transfer of ^{252}Cf onto the fission chamber (0.05%–0.4% [5,7,30]) and the half-life of the isotope in question (0.01–0.15% [5–7]). A medium-range correlation of δc_f between different experiments is assumed in Table II of [55], given its composite nature encompassing purely random as well as strongly correlated uncertainty sources.

5 Summary

Nuclear data measurements of average prompt- and total-fission neutron multiplicities fall into a few highly developed types. For each type, the sources of uncertainty have been identified and quantified by various practitioners over many years. Individual experiments, especially older ones, are not always described in as much detail on all individual uncertainty sources or corrections as needed for the nuclear-data evaluation process. Nonetheless, it is expected that measurements of a given type will be impacted by these known inaccuracies or missing uncertainties, whether reported or not. In the present work, templates of expected measurement uncertainties were established for average prompt- and total-fission neutron multiplicities. These templates list expected uncertainty sources for the manganese-bath, liquid-scintillator absolute, and ratio measurement types. They also give ranges of uncertainties for most sources and estimates of correlation coefficients between uncertainties of each source in case that some of them were not reported for a particular measurement and cannot be estimated in any other way. The uncertainty values were estimated conservatively, based on information found for ^{252}Cf, ^{235,238}U, and ^{239}Pu multiplicity measurements in their literature or respective EXFOR entries, as well as on expert judgment from experimenters. In addition to these templates, a section lists what information on the experiments is needed to include its data faithfully in the evaluation process. Future experiments need to be carefully planned, executed, and reported in order to improve nuclear data in this area; many of the corrections can be assessed experimentally and confirmed by simulation as a matter of good practice. The templates presented here serve as a reminder of what uncertainty sources and input for the evaluation should be provided.

Conflict of interests

The authors declare that they have no competing interests to report.

Funding

We gratefully acknowledge the partial support of the Advanced Simulation and Computing program at LANL. This work was supported by the US Department of Energy through the Los Alamos National Laboratory. Los Alamos National Laboratory is operated by Triad National Security, LLC, for the National Nuclear Security Administration of the US Department of Energy under Contract No. 89233218CNA000001.

Data availability statement

The data that were created associated with this manuscript are all within its main text and tables.

Author contribution statement

DN wrote the original draft, AC and SC contributed text to that. All authors reviewed and proposed edits to the manuscripts. All authors were involved in investigations and data curation associated with the article and discussions on uncertainty quantification for $\overline{\nu}$.

References

1. J.W. Boldeman, Review of $\overline{\nu}$ for ^{252}Cf and thermal neutron fission, in *Proc. of Neutron Standards and Applications Sympos., Gaithersburg, USA* (1977), pp. 182–192
2. R.R. Spencer, R. Gwin, R. Ingle, A measurement of the average number of prompt neutrons from spontaneous fission of Californium-252, Nucl. Sc. Eng. **80**, 603 (1982)
3. E.J. Axton, A.G. Bardell, Neutron yield from the spontaneous fission of Cf-252(nu), Metrologia **21**, 59 (1985)
4. D.W. Colvin, M.G. Sowerby, Boron Pile Nu-bar Measurements, in *Proc. of IAEA Phys. Chem. Fission Conf., Salzburg, Austria* (1965), Vol. 2, p. 25
5. B.M. Aleksandrov, E.V. Korolev, Ya.M. Kramaro *et al.*, Absolute Measurements of NU(Cf-252) by Means of Manganese Bath Method, in *Proc. of All Union Conf. on Neutron Phys., Kiev, USSR* (1980), Vol. 4, p. 119
6. J.R. Smith, S.D. Reeder, R.J. Gehrke, Absolute measurement of Nu-bar for Cf-252, Electric Power Res. Inst., Nucl. Phys. Ser. **3436**, 1, (1984)
7. A. DeVolpi, K.G. Porges, Neutron yield of ^{252}Cf based on absolute measurement of the neutron rate and fission rate, Phys. Rev. C **1**, 683 (1970)
8. Z. Huan-Qiao, L. Zu-Huz, The measurement of the average number of prompt neutrons and the distribution of prompt neutron numbers for Cf-252 spontaneous fission, Chin. J. Nucl. Phys. **1**, 9 (1979)
9. H. Bozorgmanesh, G.F Knoll, Absolute measurement of the number of neutrons per spontaneous fission of ^{252}Cf, Trans. Amer. Nucl. Soc. **27**, 864 (1977)
10. A.D. Carlson et al., Evaluation of the neutron data standards, Nucl. Data Sheets **148**, 143 (2018)
11. E.J Axton, *Evaluation of the Thermal Constants of* ^{233}*U,* ^{235}*U,* ^{239}*Pu and* ^{241}*Pu, and the Fission Neutron Yield of* ^{252}*Cf*, Central Bureau for Nuclear Measurements (Geel) Report GE/PH/01/86, 1986
12. J.W. Boldeman, M.G. Hines, Prompt neutron emission probabilities following spontaneous and thermal neutron fission, Nucl. Sci. Eng. **91**, 114 (1985)
13. J.W. Boldeman, R.L. Walsh, The energy dependence of $\overline{\nu}_p$ for neutron induced fission of ^{235}U below 2.0 MeV, J. Nucl. Energy **24**, 191 (1970)
14. B.C. Diven, H.C. Martin, R.F. Taschek, Multiplicities of fission neutrons, Phys. Rev. **101**, 1012 (1956)
15. J.C. Hopkins, B.C. Diven, Prompt neutrons from fission, Nucl. Phys. **48**, 433 (1963)
16. D.S. Mather, P. Fieldhouse, A. Moat, Measurement of prompt $\overline{\nu}_{\rm tot}$ for the neutron-induced fission of Th^{233}, U^{233}, U^{234}, U^{238} and Pu^{239}, Nucl. Phys. A **66**, 149 (1965)
17. L.I. Prokhorova et al., Yield of prompt neutrons $\overline{\nu}_{\rm tot}$ in the fission of U^{235} by neutrons with energies up to 1.5 MeV, Atomnaya Énergiya **30**, 250 (1971)
18. K.E. Bolodin et al., Average number of prompt neutrons in Pu^{239} fission, Atomnaya Énergiya **33**, 901 (1972)
19. M. Soleihac, J. Frehaut, J. Gauriau, Energy dependence of $\overline{\nu}_p$ for neutron-induced fission of ^{235}U, ^{238}U and ^{239}Pu from 1.3 to 15 MeV, J. Nucl. Energy **23**, 257 (1969)
20. J. Frehaut, G. Mosinski, M. Soleihac, Recent Results in $\overline{\nu}_p$ Measurements between 1.5 and 15 MeV, in *Proc. of Topical Conference on* $\overline{\nu}_p$*. The Average Number of Neutrons Emitted in Fission, France*, Report EANDC(E)-15 "U" (1973)
21. R. Gwin, R.R. Spencer, R.W. Ingle, Measurements of the energy dependence of prompt neutron emission from ^{233}U, ^{235}U, and ^{239}Pu for $E_n = 0.0005$ to 10 MeV relative to emission from spontaneous fission of ^{252}Cf, Nucl. Sci. Eng. **94**, 365 (1986)
22. R. Gwin, R.R. Spencer, R.W. Ingle, Measurements of the energy dependence of prompt neutron neutron emission from ^{233}U, ^{235}U, ^{239}Pu, and ^{241}Pu for $E_n = 0.0005$ to 10 eV relative to emission from spontaneous fission of ^{252}Cf, Nucl. Sci. Eng. **87**, 381 (1984)
23. R. Gwin et al., *Measurements of the Average Number of Prompt Neutrons Emitted per Fission of* ^{239}*Pu and* ^{235}*U* (Oak Ridge National Laboratory ORNL/TM-6246, 1978)
24. M. Soleihac et al., Average number of prompt neutrons and relative fission cross-sections of U-235 and Pu-239 in the 0.3 to 1.4 MeV range, in *Proc. of the Conference for Nuclear Data for Reactors, Helsinki, Sweden* (1970), Vol. 2, pp. 145–156
25. J.W. Boldeman, J. Fréhaut, R.L. Walsh, A reconciliation of measurements of $\overline{\nu}_p$ for neutron-induced fission of Uranium-235, Nucl. Sci. Eng. **63**, 430 (1977)
26. M.V. Savin et al., *The Average Number of Prompt Neutrons in Fast Neutron Induced Fission of U-235, Pu-239 and Pu-240*, International Atomic Energy Agency Report IAEA-CN-26/40, 1970
27. I. Asplund-Nilsson, H. Conde, N. Starfelt, An Absolute Measurement of Nu-bar of Cf-252, Nucl. Sc. Eng. **16**, 124 (1963).
28. B.C. Diven, J.C. Hopkins, Numbers of prompt neutrons per fission for U233, U235, Pu239 and Cf252, in *Proc. of Reactor Physics Sem., Vienna, Austria* (1961), Vol. 1, p. 149
29. G. Edwards, D.J.S. Findlay, E.W. Lees, Measurements of prompt nu-bar and variance for the spontaneous fission of Cf-252 and Pu-242, Ann. Nucl. Energy **9**, 127 (1982)
30. P.H. White, E.J. Axton, Measurement of the number of neutrons per fission for Cf-252, J. Nucl. Energy **22**, 73 (1968)
31. Experimental Nuclear Reaction Data Library (EXFOR), IAEA Nuclear Data Section. See https://www-nds.iaea.org/exfor (accessed on 2016-8-11), or for the NNDC at Brookhaven National Laboratory, the mirror site is http://www.nndc.bnl.gov/exfor (accessed on 2016-8-11)

32. N. Otuka et al., Towards a more complete and accurate experimental nuclear reaction data library (EXFOR): international collaboration between nuclear reaction data centres (NRDC), Nucl. Data Sheets **120**, 272 (2014)
33. V.V. Zerkin, B. Pritychenko, The experimental nuclear reaction data (EXFOR): extended computer database and web retrieval system, Nucl. Instrum. Meth. Phys. Res. Sec. A **888**, 31 (2018)
34. H. Condé, J. Hansén, M. Holmberg, Prompt $\overline{\nu}_{\rm tot}$ in Neutron-induced Fission of ^{239}Pu and ^{241}Pu, J. Nucl. Energy **22**, 53 (1968)
35. Z. Huanqiao et al., The dependence of average numbers of prompt fission neutron of Pu-239 on incident fast neutron energies, Chin. J. Nucl. Phys. **2**, 29 (1980)
36. B. Nurpeisov et al., Dependence of $\overline{\nu}_{\rm tot}$ on neutron energies up to 5 MeV for ^{233}U, U^{235}, and ^{239}Pu, Atomnaya Énergiya **39**, 199 (1975)
37. G.N. Smirenkin et al., Mean number of prompt neutrons in the fission of U^{233}, U^{235}, Pu^{239} by 4 and 15 MeV neutrons, Sov. At. Energy **4**, 253 (1958)
38. R.L. Walsh, J.W. Boldeman, The energy dependence of $\overline{\nu}_p$ for ^{233}U, ^{235}U and ^{239}Pu below 5.0 MeV, J. Nucl. Energy **25**, 321 (1971)
39. I. Johnstone, *A Measurement of the Average Number of Prompt Neutrons Emitted in Fission at High Energy*, Atomic Energy Research Establishment Report A.E.R.E NP/R 1912, 1956
40. V.I. Kalashnikova et al., Absolute evaluation of the average number of neutrons emitted in the fission of some isotopes of uranium and plutonium, in *Proc. of the USSR Conf. peaceful Uses of Atomic Energy, USSR* (1955), Vol. 1955, p. 156
41. M.V. Savin et al., Energy dependence of $\overline{\nu}_{\rm tot}$ in the fission of U^{235} by fast neutrons, Sov. J. Nucl. Phys. **16**, 638 (1973)
42. P.J. Leroy, Nombres moyens de neutrons prompts Èmis dans La fission de ^{238}U, ^{239}Pu, ^{232}Th, Le Journal de Physique et le Radium **21**, 617 (1960)
43. E. Fort, J. Freehaut, H. Tellier, P. Long, Evaluation of $\overline{\nu}_p$ for ^{239}Pu: impact for applications of the fluctuations at low energy, Nucl. Sci. Eng. **99**, 375 (1988)
44. J.E. Lynn, P. Talou, O. Bouland, Reexamining the role of the (n,γf) process in the low-energy fission of ^{235}U and ^{239}Pu, Phys. Rev. C **97**, 064601 (2018)
45. E.J. Axton, Accuracies and correction in the neutron bath techniques, in *Proc. of Neutron Standards and Applications Sympos., Gaithersburg, USA* (1977), pp. 237–243
46. S. Croft, A. Favalli, R.D. McElroy, Jr., A review of the prompt neutron Nu-bar value for ^{252}Cf spontaneous fission, Nucl. Instrum. Meth. Phys. Res. A **954**, 161605 (2020)
47. N.J. Roberts, *MCNP Calculations of Correction Factors for Radionuclide Neutron Source Emission Rate Measurements using the Manganese Bath*, National Physical Laboratory Report ISSN 1369-6793, 2001
48. S. Croft, A. Favalli, How the choice of data reduction can strongly influence uncertainty assessment: a Re-analysis of Mn-bath experiments, Rad. Meas. **47**, 481 (2012)
49. C. De Saint Jean (co-ordinator), R.D. McKnight (Monitor), *Co-ordinated Evaluation of Plutonium-239 in the Resonance Region*, Nuclear Energy Agency WPEC report NEA/NSC/WPEC/DOC(2014)447, 2014
50. M. Divadeenam, J.R. Stehn, A least-squares evaluation of thermal data for fissile nuclei, Ann. Nucl. Energy **11**, 375 (1984)
51. J. Taieb, T. Granier, T. Ethvignot, Measurement of the average energy and multiplicity of prompt-fission neutrons from ^{238}U(n,f) and ^{237}Np(n,f) from 1 to 200 MeV, in *Proceedings of International Conference on Nuclear Data for Science and Technology, Nice, France* (2008), Vol. 114, pp. 429–432, https://doi.org/10.1051/ndata:07676
52. V.N. Nefedov, B.I. Starostov, A.A. Boytsov, *Precision Measurements of ^{252}Cf, ^{233}U, ^{235}U and ^{239}Pu Prompt Fission Neutron Spectra (PFNS) in the Energy Range 0.04–5 MeV*, IAEA Report INDC(CCP)-0457, 2014; translation into English from: in *Proc. of the All-Union Conf. on Neutron Physics, Kiev, USSR* (1983), Vol. 2, pp. 285–289, EXFOR-No. 40871.009 for ^{239}Pu and 40871.007 for ^{235}U
53. R. Capote et al., Prompt fission neutron spectra of actinides, Nucl. Data Sheets **131**, 1 (2016)
54. P. Marini et al., Energy dependence of prompt fissions neutron multiplicity in the ^{239}Pu(n,f) reaction, Phys. Lett. B **835**, 137513 (2022)
55. D. Neudecker et al., Templates of expected measurement uncertainties for prompt fission neutron spectra, EPJ Nuclear Sci. Technol. **9**, 32 (2023)
56. J.W. Boldeman, J. Fréhaut, The foil thickness correction in $\overline{\nu}_{\rm tot}$ measurements and the $(\overline{\nu}\eta)$ discrepancy, Nucl. Sci. Eng. **76**, 49 (1980)
57. D.A. Brown et al., ENDF/B-VIII.0: The 8th major release of the nuclear reaction data library with CIELO-project cross sections, new standards and thermal scattering data, Nucl. Data Sheets **148**, 1 (2018)
58. C. Wagemans, *The Nuclear Fission Process* (CRC Press Boca Raton, 1991)
59. D.L. Duke et al., Fission-fragment properties in ^{238}U(n,f) between 1 and 30 MeV, Phys. Rev. C **94**, 054604 (2016)
60. A. Tudora, Systematic behaviour of the average parameters required for the los alamos model of prompt neutron emission, Ann. Nucl. Energy **36**, 72 (2009)
61. J. Bess, editor, *International Handbook of Evaluated Criticality Safety Benchmark Experiments (ICSBEP)*, Organization for Economic Co-operation and Development-Nuclear Energy Agency Report NEA/NSC/DOC(95)03, 2019
62. D. Neudecker, ARIADNE–A program estimating covariances in detail for neutron experiments, EPJ Nuclear Sci. Technol. **4**, 34 (2018)
63. R.E. Sund, R.B. Walton, Gamma rays from short-lived fission-fragment isomers, Phys. Rev. **146**, 824 (1966)
64. J.W. Boldeman, A.W. Dalton, *Prompt Nubar Measurements for Thermal Neutron Fission*, Australian Atomic Energy Commission Report AAEC/E172, 1967
65. D.W. Colvin, The numbers of neutrons per fission, $\overline{\nu}$, from thermal to 15 MeV, in *Proc. of the Conference for Nuclear Data for Reactors, Helsinki, Sweden* (1970), Vol. 2, pp. 195–213
66. D.S. Mather, P. Fieldhouse, A. Moat, Average number of prompt neutrons from U^{235} fission induced by neutrons from thermal to 8 MeV, Phys. Rev. **133**, B1403 (1964)
67. N.J. Roberts, L.N. Jones, *Investigation of the Implications of ^{250}Cf and ^{248}Cm in ^{252}Cf neutron sources*, National Physical Laboratory Report, 2004
68. D. Neudecker et al., Evaluations of energy spectra of neutrons emitted promptly in neutron-induced fission of ^{235}U and ^{239}Pu, Nucl. Data Sheets **148**, 293 (2018)

69. M. Devlin et al., The prompt fission neutron spectrum of ^{235}U(n,f) below 2.5 MeV for incident neutrons from 0.7 to 20 MeV, Nucl. Data Sheets **148**, 322 (2018)
70. K.J. Kelly et al., Measurement of the ^{239}Pu(n,f) prompt fission neutron spectrum from 10 keV to 10 MeV induced by 1–20 MeV neutrons, Phys. Rev. C **102**, 034615 (2020)
71. P. Marini et al., Prompt fission neutrons in the ^{239}Pu(n,f) reaction, Phys. Rev. C **101**, 044614 (2020)
72. A.E. Lovell et al., Correlations between fission fragments and neutron anisotropies in neutron-induced fission, Phys. Rev. C **102**, 024621 (2020)
73. S. Halfon, New evaluation of correction factors for high precision neutron measurements using NIST manganese bath, J. Res. Nat. Inst. Stand. Technol. manuscript in preparation (2021)

Cite this article as: Denise Neudecker, Allan D. Carlson, Stephen Croft, Matthew Devlin, Keegan J. Kelly, Amy E. Lovell, Paola Marini, and Julien Taieb, Templates of expected measurement uncertainties for average prompt and total fission neutron multiplicities, EPJ Nuclear Sci. Technol. **9**, 30 (2023)